PKC412 inhibits the zinc finger 198–fibroblast growth factor receptor 1 fusion tyrosine kinase and is active in treatment of stem cell myeloproliferative disorder

Jing Chen*†, Daniel J. DeAngelo†‡, Jeffery L. Kutok§, Ifor R. Williams¶, Benjamin H. Lee*§, Martha Wadleigh‡, Nicole Duclos*, Sarah Cohen*, Jennifer Adelsperger*, Rachel Okabe*, Allison Coburn*, Ilene Galinsky‡, Brian Huntly*, Pamela S. Cohen‖, Thomas Meyer**, Doriano Fabbro**, Johannes Roesel**, Lolita Banerji‡, James D. Griffin‡, Sheng Xiao‡, Jonathan A. Fletcher‡, Richard M. Stone‡††, and D. Gary Gilliland*††

*Howard Hughes Medical Institute, Harvard Medical School, Boston, MA 02115; ‡Dana–Farber Cancer Institute, Boston, MA 02115; §Department of Pathology, Brigham and Women's Hospital, Boston, MA 02115; ¶Department of Pathology, Emory University, Atlanta, GA 30322; ‖Novartis Pharma AG, Florham Park, NJ 07932; and **Novartis Pharma AG, CH-4002 Basel, Switzerland

Edited by Owen N. Witte, University of California, Los Angeles, CA, and approved August 19, 2004 (received for review June 22, 2004)

Human stem cell leukemia–lymphoma syndrome usually presents itself as a myeloproliferative disorder (MPD) that evolves to acute myeloid leukemia and/or lymphoma. The syndrome associated with t(8;13)(p11;q12) results in expression of the ZNF198–fibroblast growth factor receptor (FGFR) 1 fusion tyrosine kinase. Current empirically derived cytotoxic chemotherapy is inadequate for treatment of this disease. We hypothesized that small-molecule inhibitors of the ZNF198–FGFR1 fusion would have therapeutic efficacy. We characterized the transforming activity of ZNF198–FGFR1 in hematopoietic cells *in vitro* and *in vivo*. Expression of ZNF198–FGFR1 in primary murine hematopoietic cells caused a myeloproliferative syndrome in mice that recapitulated the human MPD phenotype. Transformation in these assays, and activation of the downstream effector molecules PLC-γ, STAT5, and phosphatidylinositol 3-kinase/AKT, required the proline-rich domains, but not the ZNF domains, of ZNF198. A small-molecule tyrosine kinase inhibitor, PKC412 (*N*-benzoyl-staurosporine) effectively inhibited ZNF198–FGFR1 tyrosine kinase activity and activation of downstream effector pathways, and inhibited proliferation of ZNF198–FGFR1 transformed Ba/F3 cells. Furthermore, treatment with PKC412 resulted in statistically significant prolongation of survival in the murine model of ZNF198–FGFR1-induced MPD. Based in part on these data, PKC412 was administered to a patient with t(8;13)(p11;q12) and was efficacious in treatment of progressive myeloproliferative disorder with organomegaly. Therefore, PKC412 may be a useful therapy for treatment of human stem cell leukemia–lymphoma syndrome.

Recurrent translocations involving the region p11–p12 of chromosome 8 have been associated with two distinct clinical hematopoietic malignancies: acute myeloid leukemia (AML) or stem cell myeloproliferative disorder (MPD). Patients with MPD are characterized by myeloid hyperplasia with peripheral blood eosinophilia and B or T cell lymphoma. As we and others reported, the myeloid hyperplasia generally progresses to acute myeloid leukemia within a year of the original diagnosis, and a cure requires allogeneic stem cell transplantation (1, 2).

Positional cloning of recurrent chromosomal translocations associated with the MPD has demonstrated frequent involvement of the *FGFR1* gene on 8p11.2–11.1, encoding a receptor tyrosine kinase that is normally activated by fibroblast growth factors. To date, four different translocations have been described, including t(8;13)(p11;q12), t(8;9)(p11;q33), t(6;8)(q27;p11), and t(8;22)(p11;q11), which result in fusion of distinct partners to fibroblast growth factor receptor (FGFR) 1, including ZNF198 (3), CEP110 (4), FOP (5), and BCR (6), respectively. In each case, an N-terminal partner containing self-association motif is fused to the C-terminal tyrosine kinase domain of FGFR1. Recently, a fifth translocation, t(8;19)(p12;q13.3), associated with this syndrome has been cloned, and it results in an N-terminal portion of the human endogenous retrovirus gene (HERV-K) fused in frame to the C-terminal FGFR1 kinase domain (7). Although the transforming properties of HERV-K–FGFR1 have not been characterized, the other four FGFR1 fusion proteins are constitutively active tyrosine kinases and transform Ba/F3 murine hematopoietic cells to IL-3-independent growth (8–11). In addition, expression of ZNF198–FGFR1 results in increased tyrosine phosphorylation of STAT1 and STAT5 in Ba/F3 cells (10), and the FOP–FGFR1 fusion induces cell survival by activating the PLC-γ, mitogen-activated protein kinase/extracellular regulated kinase, and phosphatidylinositol 3-kinase (PI3K)/protein kinase B/molecular target of rapamycin pathways (11). These findings indicate that activation of FGFR1 tyrosine kinase and its downstream-signaling pathways play an essential role in pathogenesis of MPD induced by distinct FGFR1 fusion proteins.

ZNF198 is widely expressed and has two isoforms that contain either 4 or 10 atypical zinc fingers, a proline-rich domain, and an acidic domain. The ZNF198–FGFR1 fusion protein incorporates an intact FGFR1 C-terminal tyrosine kinase domain fused to N-terminal ZNF198 zinc fingers and proline-rich domains. ZNF198–FGFR1 is predominantly cytoplasmic (8) and activated by constitutive oligomerization (9).

We report that ZNF198–FGFR1 induces a myeloproliferative phenotype in a murine bone marrow transplant (BMT) assay, and the ZNF198 proline-rich domain is essential for transforming activity *in vivo*. We tested the potential therapeutic utility of the small-molecule tyrosine kinase inhibitor PKC412 as an option for treatment of ZNF198–FGFR1-associated MPD. PKC412 is a potent inhibitor of several kinases, including FLT3 (12–14), and is currently being evaluated in a phase II clinical trial for AML patients with and without FLT3 activating mutations.‡‡§§ PKC412 also has inhibitory activity for FGFR family members and was therefore tested for ZNF198–FGFR1 inhibitory activity *in vitro* and *in vivo* as well as in a patient with ZNF198–FGFR1-associated MPD.

This paper was submitted directly (Track II) to the PNAS office.

Abbreviations: AML, acute myelogenous leukemia; BMT, bone marrow transplant; FGFR, fibroblast growth factor receptor; MPD, myeloproliferative disorder; PI3K, phosphatidylinositol 3-kinase.

†J.C. and D.J.D. contributed equally to this work.

††To whom correspondence may be addressed. E-mail: ggilliland@rics.bwh.harvard.edu or rstone@partners.org.

‡‡Stone, R. M., Klimek, V., DeAngelo, D. J., Nimer, S., Estey, E., Galinsky, I., Neuberg, D., Yap, A., Fox, E. A., Gilliland, D. G. & Griffin, J. (2003) *Blood* **100,** 86a (abstr.).

§§Estey, E. H., Fisher, T., Giles, F., Feldman, E. J., Ehninger, G., Schiller, G. J., Klimek, V. M., Nimer, S. D., De Angelo, D. J., Gilliland, D. G., *et al.* (2003) *Blood* **102,** 614a (abstr.).

Materials and Methods

DNA Constructs. The complete ZNF198–FGFR1 cDNA and truncated ZNF198–FGFR1 constructs were generated and subcloned into retroviral vectors MSCV-neoEB and MSCV2.2IRESGFP as described in ref. 9.

Cell Cultures, Retrovirus Production, and Ba/F3 Cell IL-3 Independence Proliferation Assays. Ba/F3 cells were cultured in RPMI medium 1640 with 10% FBS and 1.0 ng/ml IL-3 (R & D Systems). The 293T cells were cultured in DMEM with 10% FBS. The retroviral stocks were generated, and the viral titers were determined as described in refs. 15 and 16. For the murine BMT assays, the viral titers of all constructs were normalized to 1×10^6 infectious units/ml. Ba/F3 cell lines stably expressing ZNF198–FGFR1 variants were generated, and IL-3-independent growth was assayed as described in ref. 17. For cell viability assays, 1×10^5 Ba/F3 cells were cultured in 24-well plates with increasing concentrations of PKC412 in the absence of IL-3. The relative cell viability at each experimental time point was determined by using the Celltiter96AQ$_{\text{ueous}}$ One solution proliferation kit (Promega).

Western Blotting and RT-PCR. When assayed for phosphorylation levels of different protein factors, Ba/F3 cells were either serum starved or, in some experiments, treated with PKC412 for 4 h before being lysed. The cell extracts were analyzed by enzyme-linked immunoblotting. Antibodies included rabbit antibodies recognizing FGFR1, STAT5b, phospho-PI3K-p85 (Tyr-508) (Santa Cruz Biotechnology), mouse 4G10 antiphosphotyrosine antibody (Upstate Biotechnology, Lake Placid, NY), and rabbit antibodies recognizing phospho-STAT5 (Tyr-694), PLC-γ1, and phospho-PLC-γ1 (Tyr-783) (Cell Signaling Technology, Beverly, MA). RT-PCR analysis of RNA derived from patient bone marrow samples was performed as described in ref. 3.

Murine BMT Assay and PKC412 Treatment of the Animals. The murine BMT assays and drug treatment were performed as described in refs. 18 and 19. Bone marrow cells (1×10^6) transduced with distinct retroviral constructs were injected into the lateral tail veins of lethally irradiated (450 cGy $\times$ 2) syngeneic BALB/c recipient mice. For secondary transplantation, 1×10^6 spleen cells from primary recipients were injected into sublethally irradiated (450 cGy $\times$ 1) hosts. For Southern blotting analysis, genomic DNA was purified by using a PUREGENE DNA isolation kit (Gentra Systems). DNA (10 μg) was digested with *Eco*RI, electrophoretically separated on a 0.8% agarose gel, and transferred to Hybond-*n* + nylon membranes (Amersham Biosciences). The enhanced GFP probe was prepared by restriction digestion from MSCV2.2IRESGFP vector with *Nco*I and *Sal*I and labeled with ^{32}P by random priming with RadPrime (Invitrogen).

PKC412 was prepared as 6% wt/wt stock in Gelucire 44/14 (GC) (Gattefosse, Saint-Priest Cedex, France) and diluted with sterile deionized water before administration. Dosing of PKC412 (100 mg/kg per day) was performed every 24 h by oral gavage as described in ref. 18. Placebo group of mice received equal volume of GC solution. Diseased animals were identified by splenomegaly or moribund appearance and were killed for further analyses. Histopathological analyses were performed; single-cell suspensions of bone marrow, spleen, and peripheral blood were analyzed by flow cytometric analysis as described in ref. 15. Statistical significance for survival analysis was assessed by using the log-rank test.

PKC412 Clinical Trial. A t(8;13)(p11;q12) patient with progressive myeloproliferative disorder was treated with PKC412. Protocol Dana–Farber Cancer Institute 03-112 (Novartis CPKC412A2104) is a randomized phase IIb clinical trial designed to test the safety and efficacy of two doses of PKC412 (50 and 100 mg orally twice a day) in patients with relapsed or refractory AML, previously untreated AML not deemed a chemotherapy candidate, or myelodysplastic syndrome or variants (14). The protocol was carried out and approved by the Institutional Review Board at the Dana–Farber Cancer Institute (principal investigator: Richard M. Stone). Other eligibility requirements included Eastern Cooperative Oncology Group performance status 0-2, creatinine $<$2.0 g/dl, normal liver function tests, and no major comorbid disease. The patient must have recovered from prior cytotoxic therapy; hydroxyurea was not allowed at any time after 7 days before the start of protocol therapy. Patients received their assigned dose of PKC412 daily until progression or the occurrence of grade 3 or greater nonhematological toxicity. Assessment of response and toxicity was carried out by weekly visits for physical examination and blood testing and by monthly bone marrow examinations. Ancillary studies included serial blood tests for pharmacodynamics (including tyrosine kinase autophosphorylation studies as described) and pharmacokinetics.

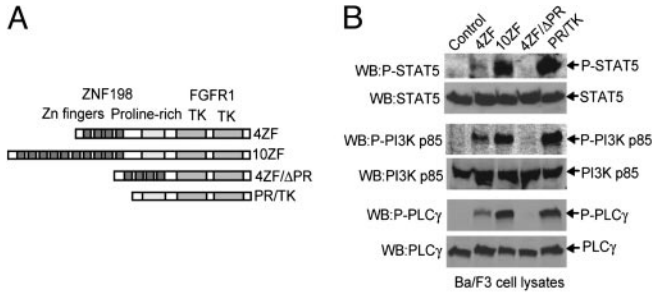

Fig. 1. The ZNF198–FGFR1 fusion requires the ZNF198 proline-rich domain for kinase activation and transformation of Ba/F3 cells. (*A*) Schematic diagram of ZNF198–FGFR1 fusion proteins and truncation constructs. (*B*) ZNF198–FGFR1 fusion requires a ZNF198 proline-rich domain to activate downstream signaling intermediates. Ba/F3 cells stably expressing ZNF198–FGFR1 variants were lysed, and tyrosine phosphorylation of STAT5, PI3K, and PLC-γ were detected by Western blot analysis.

Results

ZNF198–FGFR1 Requires the ZNF198 Proline-Rich Domain for Kinase Activation and Transformation in Ba/F3 Cells. We evaluated the transforming properties of two ZNF198–FGFR1 variants cloned from stem cell MPD patients with t(8;13)(p11;q12) and related mutants in Ba/F3 cells. These variants included two isoforms of ZNF198–FGFR1 (4ZF and 10ZF, containing 4 and 10 N-terminal zinc fingers, respectively), as well as two truncation mutants, 4ZF/ΔPR and PR/TK (Fig. 1*A*). 4ZF/ΔPR was comprised of four ZNF198 zinc fingers directly fused to the FGFR1 tyrosine kinase by deletion of the ZNF198 proline-rich domain from 4ZF, whereas PR/TK lacked all ZNF198 zinc fingers but retained the ZNF198 proline-rich domain (Fig. 1*A*).

Each ZNF198–FGFR1 isoform or mutant was subcloned into retroviral vectors carrying a neomycin resistance gene and stably transduced in Ba/F3 murine hematopoietic cells. Stable Ba/F3 cell lines were assessed for IL-3-independent growth as a surrogate for transformation. As reported in ref. 9, WT ZNF198–FGFR1 isoforms 4ZF and 10ZF, as well as truncation mutant PR/TK, conferred Ba/F3 cells to IL-3 independence, whereas the control Ba/F3 cells transduced with empty vector underwent apoptotic cell death in the absence of IL-3. In contrast, cells transduced with 4ZF/ΔPR mutant had a significantly slower proliferative rate, compared with cells expressing 4ZF, 10ZF, or PR/TK (Fig. 6*A*, which is published as supporting information on the PNAS web site). Deletion of the proline-rich domain in the 4ZF/ΔPR resulted in loss of tyrosine kinase activity (Fig. 6*B*). These data indicate that the ZNF198 proline-rich domain

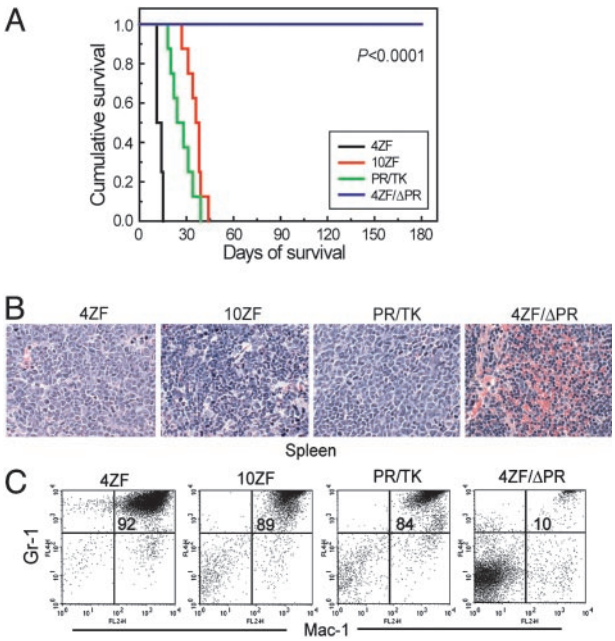

Fig. 2. ZNF198–FGFR1 induces a fatal myeloproliferative disorder in a murine BMT model. (*A*) Kaplan–Meier survival plot of mice transplanted with bone marrow cells transduced by ZNF198–FGFR1. (*B*) Histopathologic tissue sections from representative mice stained with hematoxylin/eosin (×400 magnification). Spleen of the mouse transduced by each ZNF198–FGFR1 construct except the kinase-inactive 4ZF/ΔPR demonstrates marked expansion of maturing myeloid elements, many with folded or ring-like nuclei, and small numbers (<5%) of blast forms, compatible with a myeloproliferative disorder. (*C*) Flow cytometry analysis of peripheral blood cells from representative mice. The immunophenotype illustrates a high percentage of mature myeloid cells (identified as Gr-1 and Mac-1 double-positive cells) in peripheral blood of 4ZF, 10ZF, and PR/TK mice but not in 4ZF/ΔPR mice. The percentage of Gr-1+/Mac-1+ granulocytes in the upper-right quadrant of the dot plots is indicated.

is essential for ZNF198–FGFR1 kinase activity and transforming activity in Ba/F3 cells.

Native FGFR1, when stimulated by FGF ligand, activates multiple downstream signaling components including STATs, PI3K, PLC-γ, and mitogen-activated protein kinase (20, 21). In consonance with the data on tyrosine kinase activity and transformation of Ba/F3 cells, the 4ZF and 10ZF ZNF198–FGFR1 isoforms and the PR/TK mutant activated a similar spectrum of signaling intermediates as assessed by phosphorylation of STAT5, PI3K, and PLC-γ, whereas the 4ZF/ΔPR mutant did not (Fig. 1*B*).

ZNF198–FGFR1 Variants 4ZF, 10ZF, and PR/TK but Not 4ZF/ΔPR Induce a Myeloproliferative Disorder in a Murine BMT Assay. We next tested the *in vivo* activity of ZNF198–FGFR1 constructs in primary hematopoietic cells in a murine BMT assay. Animals receiving bone marrow cells transduced by 4ZF, 10ZF, or PR/TK developed a myeloproliferative disorder with many of the phenotypic characteristics of the human MPD, including peripheral blood leukocytosis and splenomegaly due to extramedullary hematopoiesis, and were killed because of disease progression with a median latency of 11–38.5 days, (Fig. 2 and Table 1). In contrast, mice transplanted with the 4ZF/ΔPR mutant engrafted normally and survived without evidence of disease after a follow-up test >6 months later (Fig. 2 and Table 1). Southern blot analysis showed oligoclonal disease as assessed by retroviral integration in representative animals from each group (data not shown). Histopathologic examination of tissue sections showed changes consistent with the presence of a systemic MPD in mice transplanted with the 4ZF, 10ZF, or PR/TK constructs. In contrast, tissue samples from 4ZF/ΔPR mice were normal with no evidence of a myeloproliferative disorder. For example, in Fig. 2*B*, the 10ZF-transduced mice had markedly enlarged spleens with effacement of splenic architecture due to the loss of white pulp and the expansion of red pulp. These histologic changes could be attributed to extramedullary hematopoiesis dominated by mature myeloid forms and variable numbers of megakaryocytes and erythroid precursors. Bone marrow samples from 10ZF mice were markedly hypercellular with a predominance of mature myeloid forms and small numbers of erythroid and megakaryocytic elements (data not shown). 4ZF and PR/TK mice displayed a similar disease phenotype but had a slightly higher percentage of immature myeloid forms in the spleen and liver than was observed in the 10ZF mice. This difference in maturity of the atypical myeloid expansion in mice transplanted with ZNF198–FGFR1 variants suggests that although the zinc fingers are not required for self-association and kinase activation of the fusion tyrosine kinase, they may recruit or activate other factors that promote differentiation of the transformed bone marrow cells. Of particular note, one PR/TK mouse demonstrated coexistent lymphoid and myeloid disease with the presence of a markedly enlarged mesenteric lymph node infiltrated by atypical lymphoid cells. Such biphenotypic manifestations are typical of the human MPD (1, 2).

Flow cytometric analysis confirmed the myeloproliferative phenotype of diseased ZNF198–FGFR1 mice. There were abnormally elevated numbers of mature neutrophils (84–92%) that were positive for the late myeloid markers Gr-1 and Mac-1 in the peripheral blood of 4ZF, 10ZF, and PR/TK transplanted animals, compared with 10% Gr-1+/Mac-1+ cells in the blood samples of 4ZF/ΔPR mice (Fig. 2*C*). Similar results were obtained from flow cytometric analysis of spleen cells from the same representative mice (data not shown).

These data indicate that ZNF198–FGFR1 fusion proteins predominantly induce a myeloproliferative disorder phenotype in primary hematopoietic cells in mice and that the ZNF198 proline-rich domain, but not the zinc finger domain, is required. We further tested the spleen cells from diseased 4ZF, 10ZF, and PR/TK transplanted mice for serial transplantability in a secondary recipient. None of the recipient mice developed myeloid or lymphoid disease after transplantation of 1 million cells by tail vein injection into sublethally irradiated syngeneic recipients (450 cGy) (data not shown).

PKC412 Inhibits ZNF198–FGFR1 Fusion Tyrosine Kinases. Enzymatic assays had previously demonstrated inhibitory activity of

Table 1. Analyses of mice transplanted with distinct ZNF198–FGFR1 variants

Variant	No. diseased/no. transplanted	Latency/median, days	WBC count/median, 10^6/ml	Spleen weight/median, mg
4ZF	8/8	11–15/11	42–496/252	364–872/416
10ZF	8/8	27–44/38.5	30–106/47	308–646/476
PR/TK	8/8	18–39/29	17–356/60	239–1,502/660
4ZF/ΔPR	0/11	>180	<3.5	<95

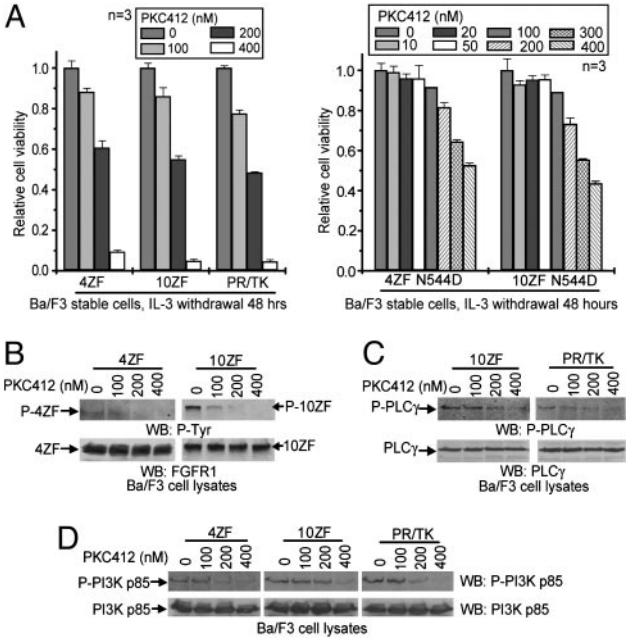

Fig. 3. PKC412 inhibits ZNF198–FGFR1 variants *in vitro*. (*A*) Dose–response analysis of Ba/F3 cells stably expressing 4ZF, 10ZF, or PR/TK constructs to PKC412 (*Left*). Mutation N544D in 4ZF or 10ZF confers drug resistance to PKC412 (*Right*). The relative viability was normalized to the viability of cells in the absence of PKC412. (*B*) PKC412 inhibits autophosphorylation of ZNF198–FGFR1. Tyrosine-phosphorylated FGFR1 was assessed by using antiphosphotyrosine antibody 4G10, whereas control ZNF198–FGFR1 protein was probed by a FGFR1 antibody. (*C* and *D*) PKC412 abrogates ZNF198–FGFR1-dependent phosphorylation of downstream signaling components PLC-γ and PI3K.

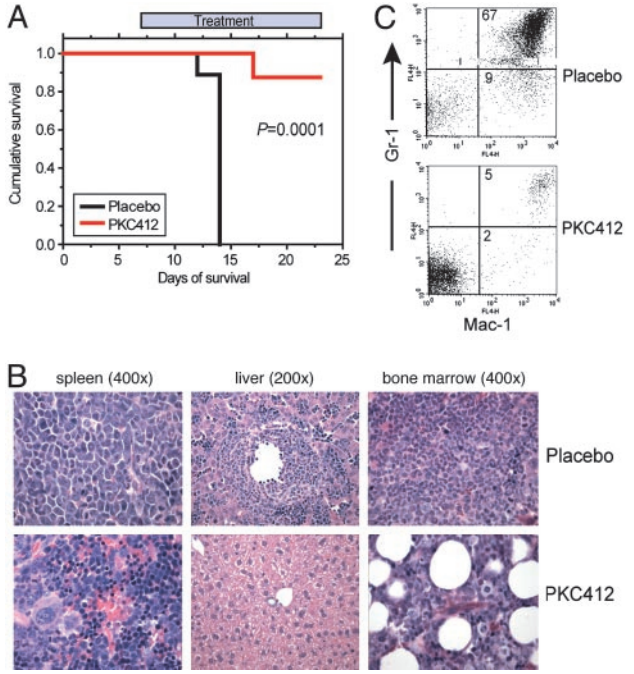

Fig. 4. PKC412 increases survival in a murine BMT model of MPD induced by the ZNF198–FGFR1 4ZF. (*A*) Kaplan–Meier plot shows the survival of mice transplanted with bone marrow cells expressing ZNF198–FGFR1 4ZF that were treated with either placebo or PKC412. (*B* and *C*) Histopathology and immunophenotypic analysis of the spleen, liver, and bone marrow of placebo- and PKC412-treated mice at time of sacrifice or study endpoint. Marked expansion of maturing myeloid elements was observed, many with folded or ring-like nuclei, in the liver and spleen of placebo-treated animals. Efficacy is demonstrated in part by showing a significant reduction in myeloid lineage infiltration in liver (*B Center*) or spleen (*B Left*) of PKC412-treated mice, and by marked reduction of Gr-1/Mac-1 positive cells in the spleen of PKC412-treated mice (*C Lower*).

PKC412 for purified FGFR family members. To determine whether PKC412 inhibits ZNF198–FGFR1, we performed a dose–response analysis of Ba/F3 cells stably expressing the 4ZF, 10ZF, or PR/TK mutants. PKC412 effectively inhibited the growth of ZNF198–FGFR1-transformed Ba/F3 cells in the absence of IL-3 with a cellular IC_{50} of ≈200 nM (Fig. 3*A*). Because PKC412 is a selective rather than specific inhibitor, we next tested for the specificity of PKC412 for ZNF198–FGFR1 inhibition. Exposure of cells stably transduced with an empty vector control growing in the presence of IL-3 to increasing concentrations of PKC412 revealed a >50-fold shift in the IC_{50}, compared with ZNF198–FGFR1-transformed cells, consistent with a specific effect of PKC412 (data not shown). To further confirm specificity, we introduced an N544D mutation in the context of FGFR1 into ZNF198–FGFR1 4ZF and 10ZF fusion proteins, corresponding to a N659D mutation in the context of PDGFRα that confers PKC412 resistance to the FIP1L1–PDGFRα fusion tyrosine kinase (18). Ba/F3 cells transformed with 4ZF N544D or 10ZF N544D demonstrated resistance to PKC412, with an elevated cellular IC_{50} of ≈2-fold (Fig. 3*A*). Taken together, these data indicate that ZNF198–FGFR1 is the target for inhibition of Ba/F3 cells by PKC412. Moreover, these data also correlate with the observations that PKC412 inhibited ZNF198–FGFR1 tyrosine autophosphorylation as well as phosphorylation of ZNF198–FGFR1 signaling intermediates, including PLC-γ and PI3K (Fig. 3 *B–D*).

PKC412 Is Effective for the Treatment of ZNF198–FGFR1-Induced Myeloproliferative Disorder in a Murine Model. The murine BMT disease model of ZNF198–FGFR1-induced MPD provided a model system to test the efficacy of PKC412. The BMT assay was repeated by using the ZNF198–FGFR1 4ZF construct, and recipient mice were divided into two groups that were treated with daily oral gavage of vehicle control or PKC412 (100 mg/kg per day), respectively. The animals in the control group receiving placebo developed myeloproliferative disorder as observed previously, characterized by splenomegaly and marked leukocytosis, and were all killed by day 13 posttransplantation (Fig. 4*A* and Table 2). Mice in the PKC412 group were treated with the drug for 1 week after all of the placebo-treated animals were killed because of disease progression. There was a statistically significantly prolonged survival in the PKC412-treated mice, with seven of eight mice in this group alive at the study endpoint (day 24) ($P = 0.0001$, Fig. 4*A*). These mice also had markedly reduced spleen weights and WBC counts (Table 2). Similar data were obtained with PKC412 treatment of disease induced by the

Table 2. Efficacy of PKC412 for the treatment of 4ZF- or 10ZF-induced myeloproliferative disorder

	Placebo	PKC412
4ZF BMT mice		
Spleen weight/median, mg	389–568.4/460.1	27–204.6/93.4
WBC count/median, 10^6/ml	45.25–265/136	0.96–11.07/3
n	9	8
10ZF BMT mice		
Spleen weight/median, mg	361–822/522.1	28–122/83.5
n	11	10
WBC count/median, 10^6/ml	91.02–227.4/122	0.87–3.31/2.34
n	11	7

n, number of animals.

ZNF198–FGFR1 10ZF isoform (Table 2). Efficacy of PKC412 was confirmed by histopathologic examination showing marked reduction of myeloid infiltration of spleen, liver, and bone marrow and by flow cytometric analysis showing a marked decrease in the Mac-1/Gr-1 double-positive cells in the spleen from a representative PKC412-treated 4ZF mouse (5%), compared with a placebo-treated 4ZF mouse (67%) (Fig. 4 *B* and *C*). Similar histopathologic and flow cytometric data were obtained with PKC412 treatment of 10ZF isoform-induced disease (data not shown). These data indicate that PKC412 is efficacious in treatment of MPD induced by either ZNF198–FGFR1 4ZF or 10ZF *in vitro* and *in vivo*.

Activity of PKC412 in Treatment of t(8;13)(p11q;12)-Associated MPD. Based in part on these observations, a t(8;13)(p11;q12) patient with ZNF198–FGFR1-induced progressive myeloproliferative disorder was treated with PKC412. A 52-year-old woman was seen in May 2003 for preoperative evaluation of a rectocele. A complete blood count showed a leukocyte count of 37,000 per μl with 57% neutrophils, 10% band forms, 8% lymphocytes, 2% monocytes, and 11% metamyelocytes; 14.7 g/dl Hb; hematocrit of 44%; and a count of 133,000 platelets per μl. On physical examination, splenomegaly and diffuse shotty lymphadenopathy of the cervical and axillary lymph nodes were observed. Bone marrow examination showed hypercellularity with a predominance of maturing myeloid elements and <5% blast forms, consistent with a MPD (data not shown). Cytogenetics showed the t(8;13)(p11;q12) associated with the ZNF198–FGFR1 fusion. Expression of ZNF198–FGFR1 was confirmed by RT-PCR analysis of RNA derived from patient bone marrow samples (Fig. 5*B*). The BCR-ABL gene rearrangement was not detected by fluorescence *in situ* hybridization, nor was the *BCR-ABL* transcript detected by RT-PCR (data not shown). At 3 months after presentation, the patient had progressive and symptomatic lymphadenopathy of the posterior auriclar, temporal, submandibular, anterior, and posterior cervical and axillary lymph nodes. CT scan showed diffuse lymphadenopathy of the neck and significant lymphadenopathy involving the mediastinum as well as the precarinal region and retroperitoneum, and splenomegaly (14-cm cephalocaudal span) also was noted (data not shown).

The patient was treated on a randomized phase II clinical trial evaluating two doses of the oral tyrosine kinase inhibitor PKC412 in patients with both mutant and WT FLT3 myeloid malignancies not appropriate for chemotherapy. The patient received PKC412 (100 mg orally twice a day), complicated by mild nausea and anorexia without emesis during the first 2 weeks of therapy. There was a progressive reduction in peripheral blood leukocytosis (from ≈50,000 cells per μl to ≈12,000 cells per μl without hematological toxicity) (Fig. 5*A*), gradual resolution of temporal, preauricular, submandibular, anterior, posterior cervical, and axillary lymphadenopathy, and reduction in splenomegaly (data not shown). Radiographic studies performed 3 months after initiation of therapy revealed marked improvement of her cervical, mediastinal, and retroperitoneal lymphadenopathy, and marked regression of splenomegaly to normal size (10.9 × 6.7 × 11.9 cm). Monthly bone marrow examinations showed a persistently hypercellular bone marrow with a myeloid predominance, including increased number of early forms with <5% myeloblasts; all metaphases were positive for the t(8;13) (Fig. 5*D*). Western blot analysis of patient peripheral blood samples showed reduction in phosphotyrosine content of the ZNF198–FGFR1 fusion with PKC412 therapy (Fig. 5*C*). The patient remained clinically stable on PKC412 for 6 months and then went off study to undergo an allogeneic stem cell transplant.

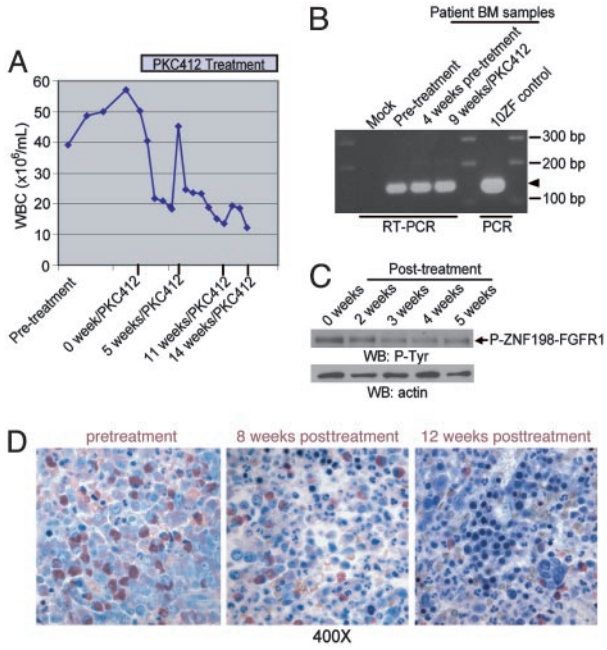

Fig. 5. Efficacy of PKC412 in treating t(8:13)p11;q12)-associated myeloproliferative disorder in humans. (*A*) Progressive reduction in peripheral blood leukocyte count before and after initiation of PKC412 therapy. The transient increase 5 weeks posttreatment was associated with a bolus of steroids given to treat an allergic reaction to i.v. contrast. (*B*) RT-PCR analysis of RNA derived from patient bone marrow samples before and during therapy with PKC412. A fragment of a 154-bp unique ZNF198–FGFR1 fusion sequence was amplified and is indicated by an arrowhead. A mock RT-PCR reaction with water instead of RNA template and a PCR reaction with plasmid-encoding 10ZF as a template were included as controls. (*C*) Western blot analysis of patient samples before and during therapy with PKC412 demonstrated progressive reduction in phosphotyrosine content of ZNF198–FGFR1. (*D*) Histopathologic examination by a standard Giemsa stain on the patient samples, which are from Zenker's fixed bone marrow core biopsy specimens before therapy with PKC412, shows a hypercellularity of immature myeloid lineage cells, increased immature granulocytic forms including eosinophils, and <5% blast forms (*Left*). Subsequent examination after initiation of therapy showed progressive increase in maturity in the myeloid lineage and normalization of the myeloid-to-erythroid ratio with corresponding increases in erythropoietic and megakaryocyte lineage cells.

Discussion

Small-molecule tyrosine kinase inhibitors are efficacious in treating certain human hematopoietic malignancies and solid tumors associated with dysregulation of tyrosine kinases. For example, imatinib (Gleevec, Novartis Pharmaceuticals, East Hanover, NJ) is effective in the clinical treatment of BCR-ABL-positive chronic myelogenous leukemia (CML), TEL-PDGFβR-induced chronic myelomonocytic leukemia (CMML), hypereosinophilic syndrome associated with the FIP1L1-PDGFRA fusion, and gastrointestinal stromal cell tumors (GIST) associated with activating mutations of c-KIT (18, 22–24). Similar strategies are being evaluated for treatment of AML associated with activating mutations in FLT3 (14, 19, §§). One of these inhibitors, PKC412, also has inhibitory activity for FGFR1. In this work, we investigated PKC412 as an option for treatment of ZNF198–FGFR1-positive MPD.

ZNF198–FGFR1 is a constitutively activated tyrosine kinase that activates downstream effectors, including STAT5, PI3K, and PLC-γ and transforms the hematopoietic cell line Ba/F3 to factor independent growth. Mutational analysis demonstrated that these activities require the ZNF198 proline-rich domain but not the zinc finger domains. Moreover, we observed that

PKC412 effectively inhibits growth of Ba/F3 cells transformed with ZNF198–FGFR1 as well as inhibiting ZNF198–FGFR1 kinase activation and downstream effectors including PI3K and PLC-γ.

To test PKC412 inhibitory efficacy *in vivo*, we developed a murine model of ZNF198–FGFR1-induced myeloproliferative disorder. In a murine-BMT assay, expression of activated ZNF198–FGFR1 variants caused a myeloproliferative phenotype in mice characterized by splenomegaly, peripheral leukocytosis comprised mainly of mature neutrophils, and extramedullary hematopoiesis in the spleen and liver. This phenotype is similar to that observed in humans with t(8;13)(p11;q12)-associated myeloproliferative disorder. In consonance with data obtained in biochemical and cell-culture assays, mice transplanted with bone marrow cells transduced by the 4ZF/ΔPR mutant did not develop disease with followup of >6 months posttransplantation. Our findings thus indicate a central role for the ZNF198–FGFR1 fusion in the induction of a myeloproliferative phenotype *in vivo*. Recent reports indicate that ZNF198–FGFR1 may also confer a predilection for development of lymphoproliferative and myeloproliferative disorder in a murine model (25), and that expression of FOP–FGFR1 in primary bone marrow cells also induces a similar fatal myeloproliferative disorder in mice (26). PKC412 was efficacious in treating ZNF198–FGFR1-induced myeloproliferative disorder in the murine model with statistically significant prolongation in survival and reduction in disease burden as assessed by complete blood counts, histopathologic analysis, and flow cytometric analysis. We also observed clinical activity of PKC412 in treatment of a patient with progressive leukocytosis, lymphadenopathy, and splenomegaly associated with t(8;13)(p11;q12) myeloproliferative disorder. Although the improvement in the patient's leukocytosis and lymphadenopathy were of a sufficient degree to ameliorate symptoms, she still had a persistent cytogenetic abnormality (Fig. 5*B*), suggesting the need of additional therapies to obtain a cytogenetic remission. Therefore, the patient underwent allogeneic stem cell transplantation.

Taken together, these data indicate that pharmacologic inhibition of ZNF198–FGFR1 with small-molecule inhibitors like PKC412 may be efficacious in treatment of t(8;13)-associated myeloproliferative disorder and perhaps for other human disorders associated with dysregulated FGFR1 activity, including overexpression or activating mutations of FGFR1 in human skeletal disorders such as Pfeiffer syndrome (27), or in human cancers, including breast cancer (28), pancreatic adenocarcinomas (29), and malignant astrocytomas (30).

We thank Alexis Bywater for administrative assistance, the Gilliland lab for valuable discussion with members, and our coinvestigators on Novartis trial CPKC412A2104: T. Fischer, University Mainz Cancer Center, Mainz, Germany; E. Feldman, Cornell University Cancer Center, New York; G. Ehninger, University Carl Gustav Carus, Dresden, Germany; G. Schiller, University of California Medical Center, Los Angeles; V. Klimek, Memorial Sloan–Kettering Cancer Center, New York; and F. Giles, M. D. Anderson Cancer Center, Houston. This work was supported in part by National Institutes of Health Grants DK50654 and CA66996, the Leukemia and Lymphoma Society, and the Doris Duke Charitable Foundation. J.C. is a fellow of the Leukemia and Lymphoma Society. D.G.G. is an investigator of the Howard Hughes Medical Institute.

1. Macdonald, D., Aguiar, R. C., Mason, P. J., Goldman, J. M. & Cross, N. C. (1995) *Leukemia* **9,** 1628–1630.
2. Inhorn, R. C., Aster, J. C., Roach, S. A., Slapak, C. A., Soiffer, R., Tantravahi, R. & Stone, R. M. (1995) *Blood* **85,** 1881–1887.
3. Xiao, S., Nalabolu, S. R., Aster, J. C., Ma, J., Abruzzo, L., Jaffe, E. S., Stone, R., Weissman, S. M., Hudson, T. J. & Fletcher, J. A. (1998) *Nat. Genet.* **18,** 84–87.
4. Guasch, G., Mack, G. J., Popovici, C., Dastugue, N., Birnbaum, D., Rattner, J. B. & Pebusque, M. J. (2000) *Blood* **95,** 1788–1796.
5. Popovici, C., Zhang, B., Gregoire, M. J., Jonveaux, P., Lafage-Pochitaloff, M., Birnbaum, D. & Pebusque, M. J. (1999) *Blood* **93,** 1381–1389.
6. Demiroglu, A., Steer, E. J., Heath, C., Taylor, K., Bentley, M., Allen, S. L., Koduru, P., Brody, J. P., Hawson, G., Rodwell, R., *et al.* (2001) *Blood* **98,** 3778–3783.
7. Guasch, G., Popovici, C., Mugneret, F., Chaffanet, M., Pontarotti, P., Birnbaum, D. & Pebusque, M. J. (2003) *Blood* **101,** 286–288.
8. Ollendorff, V., Guasch, G., Isnardon, D., Galindo, R., Birnbaum, D. & Pebusque, M. J. (1999) *J. Biol. Chem.* **274,** 26922–26930.
9. Xiao, S., McCarthy, J. G., Aster, J. C. & Fletcher, J. A. (2000) *Blood* **96,** 699–704.
10. Smedley, D., Demiroglu, A., Abdul-Rauf, M., Heath, C., Cooper, C., Shipley, J. & Cross, N. C. (1999) *Neoplasia* **1,** 349–355.
11. Guasch, G., Ollendorff, V., Borg, J. P., Birnbaum, D. & Pebusque, M. J. (2001) *Mol. Cell. Biol.* **21,** 8129–8142.
12. Fabbro, D., Ruetz, S., Bodis, S., Pruschy, M., Csermak, K., Man, A., Campochiaro, P., Wood, J., O'Reilly, T. & Meyer, T. (2000) *Anticancer Drug Des.* **15,** 17–28.
13. Andrejauskas-Buchdunger, E. & Regenass, U. (1992) *Cancer Res.* **52,** 5353–5358.
14. Weisberg, E., Boulton, C., Kelly, L. M., Manley, P., Fabbro, D., Meyer, T., Gilliland, D. G. & Griffin, J. D. (2002) *Cancer Cell* **1,** 433–443.
15. Schwaller, J., Frantsve, J., Aster, J., Williams, I. R., Tomasson, M. H., Ross, T. S., Peeters, P., Van Rompaey, L., Van Etten, R. A., Ilaria, R., Jr., *et al.* (1998) *EMBO J.* **17,** 5321–5333.
16. Liu, Q., Schwaller, J., Kutok, J., Cain, D., Aster, J. C., Williams, I. R. & Gilliland, D. G. (2000) *EMBO J.* **19,** 1827–1838.
17. Chen, J., Williams, I. R., Kutok, J. L., Duclos, N., Anastasiadou, E., Masters, S. C., Fu, H. & Gilliland, D. G. (2004) *Blood,* Epub 2004 Mar 30.
18. Cools, J., Stover, E. H., Boulton, C. L., Gotlib, J., Legare, R. D., Amaral, S. M., Curley, D. P., Duclos, N., Rowan, R., Kutok, J. L., *et al.* (2003) *Cancer Cell* **3,** 459–469.
19. Kelly, L. M., Yu, J. C., Boulton, C. L., Apatira, M., Li, J., Sullivan, C. M., Williams, I., Amaral, S. M., Curley, D. P., Duclos, N., *et al.* (2002) *Cancer Cell* **1,** 421–432.
20. Hart, K. C., Robertson, S. C., Kanemitsu, M. Y., Meyer, A. N., Tynan, J. A. & Donoghue, D. J. (2000) *Oncogene* **19,** 3309–3320.
21. Ryan, P. J. & Gillespie, L. L. (1994) *Dev. Biol.* **166,** 101–111.
22. Druker, B. J. (2003) *Semin. Hematol.* **40,** 50–58.
23. Demetri, G. D., von Mehren, M., Blanke, C. D., Van den Abbeele, A. D., Eisenberg, B., Roberts, P. J., Heinrich, M. C., Tuveson, D. A., Singer, S., Janicek, M., *et al.* (2002) *N. Engl. J. Med.* **347,** 472–480.
24. Apperley, J. F., Gardembas, M., Melo, J. V., Russell-Jones, R., Bain, B. J., Baxter, E. J., Chase, A., Chessells, J. M., Colombat, M., Dearden, C. E., *et al.* (2002) *N. Engl. J. Med.* **347,** 481–487.
25. Roumiantsev, S., Krause, D. S., Neumann, C. A., Dimitri, C. A., Asiedu, F., Cross, N. C. & Van Etten, R. A. (2004) *Cancer Cell* **5,** 287–298.
26. Guasch, G., Delaval, B., Arnoulet, C., Xie, M. J., Xerri, L., Sainty, D., Birnbaum, D. & Pebusque, M. J. (2004) *Blood* **103,** 309–312.
27. Muenke, M., Schell, U., Hehr, A., Robin, N. H., Losken, H. W., Schinzel, A., Pulleyn, L. J., Rutland, P., Reardon, W., Malcolm, S., *et al.* (1994) *Nat. Genet.* **8,** 269–274.
28. Luqmani, Y. A., Graham, M. & Coombes, R. C. (1992) *Br. J. Cancer* **66,** 273–280.
29. Kobrin, M. S., Yamanaka, Y., Friess, H., Lopez, M. E. & Korc, M. (1993) *Cancer Res.* **53,** 4741–4744.
30. Morrison, R. S., Yamaguchi, F., Bruner, J. M., Tang, M., McKeehan, W. & Berger, M. S. (1994) *Cancer Res.* **54,** 2794–2799.